IEEE Access
Multidisciplinary | Rapid Review | Open Access Journal

Received November 19, 2019, accepted December 11, 2019, date of publication December 18, 2019,
date of current version December 30, 2019.

Digital Object Identifier 10.1109/ACCESS.2019.2960602

Real-Time Angular Motion Decoupling and Attitude Updating Method of Spinning Bodies Assisted by Satellite Navigation Data

SHUANGBIAO ZHANG[1], ZHONG SU[1], AND XINGCHENG LI[2]
[1]Beijing Key Laboratory of High Dynamic Navigation Technology, Beijing Information Science and Technology University, Beijing 100101, China
[2]School of Aerospace Engineering, Beijing Institute of Technology, Beijing 100081, China

Corresponding author: Shuangbiao Zhang (zhang_shb@bistu.edu.cn)

This work was supported in part by the National Natural Science Foundation of China under Grant 61771059, in part by the Innovation Project of Beijing Municipal Education Commission under Grant KM201911232013, and in part by the Key Cultivation Project of Beijing Information Science and Technology University under Grant 5211910952.

ABSTRACT Conventional attitude algorithms have been improved for many years, but they still have attitude updating errors due to the coupling in the complicated angular motion of spinning bodies. A real-time angular motion decoupling and attitude updating method assisted by satellite navigation data is proposed in this paper. A compositive model of angular motion for spinning bodies is built to understand and analyze the trait of angular velocity. A detailed process of angular motion decoupling is addressed with the help of satellite navigation data, including a backward decoupling process and a forward decoupling angular process, to estimate angular velocity to guarantee real-time ability. A real-time attitude updating algorithm is presented in detail for determining the real attitude of spinning bodies, and the updating process of coning attitude based on rotation vector is provided. Simulations are carried out to show the coupling effect of angular motion on the conventional attitude algorithm and verify the validity of the proposed method, and flight data are used to verify the availability of engineering application. Results show that the angular motion is decoupled and attitude accuracy is improved successfully.

INDEX TERMS Spinning bodies, coning motion, angular motion decoupling, attitude updating, real-time.

I. INTRODUCTION

Spinning bodies such as rocket projectiles, guided projectiles and guided bullets have high spinning speed, which can simplify control system structures, improve aerodynamic configurations and reduce collateral damages. Spinning bodies have to experience a complicated angular motion during fight and lead to attitude error of control systems and navigation systems, which makes people struggle with it for a long time [1]. So, it is significant to understand the composition of angular motion and study the effect on attitude updating of spinning bodies.

Due to the gyroscopic inertia created by high spinning speed, spinning bodies are more likely to make coning motion while being affected by any lateral torque, and it appears to be a kind of two-axis-rotation angular motion composed of nutation and precession [2]. Coning motion is regarded as a kind of extreme environment for the reason that it forces inertial measurement systems to generate attitude error. Therefore, the corresponding angular velocity of coning motion was regarded as an important part and was deduced as a classical model to examine attitude error mechanism. For improvements of attitude algorithms, many representative optimization schemes were proposed by researchers in various works. Bortz derived the earliest updating mechanization of strapdown attitude matrix by using rotating vector [3], and Savage presented a detailed updating process of rotating vector by using Taylor series expansion [4]. Miller updated the attitude matrix by using the quaternion that was calculated by multi-subsample algorithms of rotating vector [5]. From then on, noncommutativity error as a kind of coning error attracted more attention and was discussed seriously, and different optimization algorithms were proposed successively to reduce the effect of noncommutativity error, such as two-subsamples [3], three-subsamples [5], [6], four-subsamples [7], five-subsamples [8]

The associate editor coordinating the review of this manuscript and approving it for publication was Rosario Pecora.

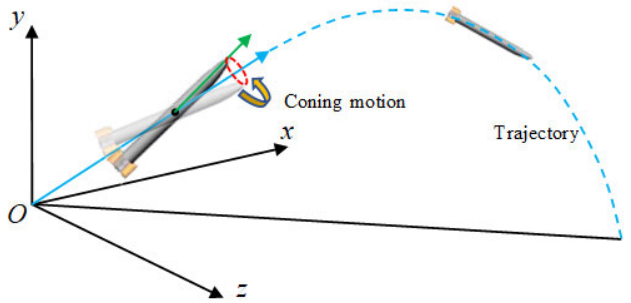

FIGURE 1. Actual angular motion of spinning bodies.

and so on. The uncompressed and compressed algorithms have the same accuracy for using multi-subsample essentially to update rotation vector, but the former has better real-time ability. Jiang used the angular velocity model of the classical coning motion to determine the coefficients of rotation vector and reduce coning error [9]. For extensive application in a stochastic coning environment, Savage developed an explicit frequency shaping method to optimize algorithm coefficients by using least-squares error minimization [10]. As noncommutativity includes many cross-product terms, Song preferred to triple-cross-product terms besides traditional terms and supplemented algorithm coefficients, which improved calculating accuracy of rotation vector and further adapted to the maneuvering environment [11], [12]. Wu proposed a RodFIter method to reconstruct incremental attitude and provided a fast approach to simplify computation complexity [13], [14]. According to analysis of rotation feature of dynamic coning motion, Zhang derived an angular motion model by defining a cone frame and cone attitude and presented an attitude calculating method [2].

So many achievements have been obtained for attitude updating algorithms up to now, but the attitude error is still induced to spinning bodies. This is because the real angular motion of spinning bodies is much more sophisticated than static or dynamic coning environment. The coupling relation of real angular motion forces attitude updating algorithms to generate coupling error by combining more than two special kinds of motion together, such as a partial dynamic coning motion superimposed on a trajectory angular motion during the whole flight in Fig. 1. The above-mentioned works pay more attention on the precision of calculating rotating vector and prefer to use coning motion simply stead of the real angular motion to verify the performance of algorithms, in spite of several coning motion models advanced [10], [11], [14]. By using current attitude algorithms, the coupled attitude is still existing because the angular velocity measured by gyroscopes is a sort of coupled data by different angular motion. Although Liu discussed an alternative to decouple a specific angular vibration, it is hard to guarantee the precision of attitude algorithm for the real flight of spinning bodies [15]. The effective way to obtain the real attitude of spinning bodies is to decouple angular motion and extract the angular velocities separately, and then update attitude in real time.

Therefore, this paper proposes a real-time angular motion decoupling and attitude updating method of spinning bodies. A necessity of common awareness is to derive angular velocity function as a model of angular motion of spinning bodies, which is not only a precondition but also a convenient way to understand the feature of angular motion and decouple it. Coning motion should be modeled to represent nutation, precession and rotation. So, the cone attitude in reference [2] is chosen, and the corresponding updating algorithm with rotation vector need be derived clearly to expand the adaptation. Additionally, position of spinning bodies from satellite navigation is brought into helping decouple angular motion and attitude in real time.

This paper is organized as follows: Section 2 builds the angular motion model of spinning bodies. A detailed process of angular motion decoupling is addressed in section 3, and a real-time attitude updating algorithm is provided in section 4. In section 5, simulations and experiments are carried out to show validity and availability of the method. The conclusions are summarized and the future work is presented in section 6.

II. COMPOSITIVE MODEL OF ANGULAR MOTION

A. MODEL OF TRAJECTORY MOTION

To describe trajectory angular motion of spinning bodies, we need define an earth frame, a trajectory frame and trajectory angles.

In the earth frame $Ox_ey_ez_e$, Ox_e axis points to the target direction, Oy_e axis is vertical to Ox_e axis in the vertical plane, and Oz_e axis is determined by the right-hand rule.

In the trajectory frame $Ox_py_pz_p$, Ox_p axis is coincident with velocity of spinning bodies, Oy_p axis is vertical to Ox_p axis in the vertical plane, and Oz_p axis is determined by the right-hand rule.

Rotation relationship between the earth frame and the trajectory frame is shown in Fig. 2, and the trajectory drift angle ψ_v and the trajectory tilt angle θ are defined.

Based on the rotation sequence from the earth frame to the trajectory frame, we obtain the trajectory transfer matrix C_e^p:

$$C_e^p = \begin{bmatrix} c\theta c\psi_v & s\theta & -c\theta s\psi_v \\ -s\theta c\psi_v & c\theta & 0 \\ s\psi_v & 0 & c\psi_v \end{bmatrix} \tag{1}$$

where the superscript p of C represents the trajectory frame, the subscript e represents the earth frame, $c(\cdot)$ represents $\cos(\cdot)$, $s(\cdot)$ represents $\sin(\cdot)$. We can derive angular velocity function ω_{ep}^p in the trajectory frame:

$$\omega_{ep}^p = \begin{bmatrix} \omega_{epx}^p \\ \omega_{epy}^p \\ \omega_{epz}^p \end{bmatrix} = \begin{bmatrix} \dot{\psi}_v \cdot c\theta \\ \dot{\psi}_v \cdot s\theta \\ \dot{\theta} \end{bmatrix} \tag{2}$$

where $\dot{\psi}_v$ and $\dot{\theta}$ are varying speeds of corresponding angles.

B. MODEL OF CONING MOTION

To describe the relationship of coning motion of spinning bodies, we need define a body frame and cone attitude.

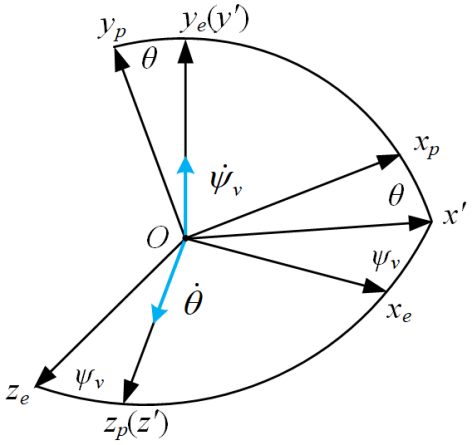

FIGURE 2. Rotation relationship between the earth frame and the trajectory frame.

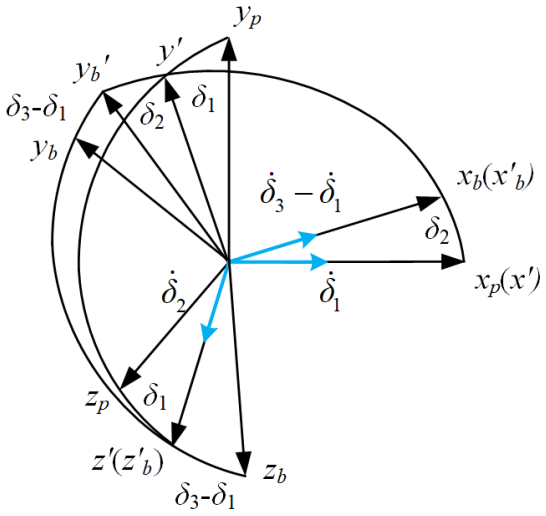

FIGURE 3. Rotation relationship between the trajectory frame and the body frame.

In the body frame $Ox_by_bz_b$, Ox_b axis is coincident with the longitudinal axis of a spinning body and points ahead, Oy_b axis is vertical to Ox_b axis in the symmetry plane of the spinning body, and Oz_b axis is determined by the right-hand rule. According to reference [2], the rotation relationship of the trajectory frame and the body frame is shown in Fig. 3, and the precession angle δ_1, the nutation angle δ_2 and the spin angle δ_3 are defined simultaneously. It needs to be noticed that the initial position of precession angle is locating of Ox_by_b in the vertical plane of the earth frame.

Based on the rotation sequence from the trajectory frame p to the body frame b, we can obtain the cone transfer matrix C_p^b:

$$C_p^b = \begin{bmatrix} c_{11} & c_{21} & c_{31} \\ c_{12} & c_{22} & c_{32} \\ c_{13} & c_{23} & c_{33} \end{bmatrix} \tag{3}$$

where the superscript b of C represents the body frame, $c_{11} = c\delta_2, c_{12} = -c(\delta_1 - \delta_3)s\delta_2, c_{13} = -s(\delta_1 - \delta_3)s\delta_2, c_{21} = c\delta_1 s\delta_2, c_{22} = s(\delta_1 - \delta_3)s\delta_1 + c(\delta_1 - \delta_3)c\delta_1 c\delta_2, c_{23} = -c(\delta_1 - \delta_3)s\delta_1 + s(\delta_1 - \delta_3)c\delta_1 c\delta_2, c_{31} = s\delta_1 s\delta_2, c_{32} = -s(\delta_1 - \delta_3)c\delta_1 + c(\delta_1 - \delta_3)s\delta_1 c\delta_2, c_{33} = c(\delta_1 - \delta_3)c\delta_1 + s(\delta_1 - \delta_3)s\delta_1 c\delta_2$.

The angular velocity function ω_{pb}^b in the body frame can be derived as:

$$\omega_{pb}^b = \begin{bmatrix} \omega_{pbx}^b \\ \omega_{pby}^b \\ \omega_{pbz}^b \end{bmatrix} = \begin{bmatrix} \dot{\delta}_1 (c\delta_2 - 1) + \dot{\delta}_3 \\ -\dot{\delta}_1 \cdot c(\delta_1 - \delta_3) \cdot s\delta_2 - \dot{\delta}_2 \cdot s(\delta_1 - \delta_3) \\ -\dot{\delta}_1 \cdot s(\delta_1 - \delta_3) \cdot s\delta_2 + \dot{\delta}_2 \cdot c(\delta_1 - \delta_3) \end{bmatrix} \tag{4}$$

where $\dot{\delta}_1, \dot{\delta}_2, \dot{\delta}_3$ are varying speeds of corresponding angles. We can use (4) to describe the changing process of coning motion and the rotating process of spinning bodies.

C. OVERALL MODEL OF ANGULAR MOTION

As we assume that the dynamic angular motion of spinning bodies is composed by trajectory motion and coning motion, the overall angle motion model, according to vector addition, can be expressed as:

$$\omega_{eb}^b = \omega_{ep}^b + \omega_{pb}^b \tag{5}$$

where ω_{ep}^b is the projected value of ω_{ep}^p in the body frame, and it can be transformed from the trajectory frame:

$$\omega_{ep}^b = C_p^b \omega_{ep}^p \tag{6}$$

III. ANGULAR MOTION DECOUPLING ASSISTED BY SATELLITE NAVIGATION DATA

A. BACKWARD DECOUPLING OF ANGULAR MOTION

Through analysis of (2), the angular velocity is a function of trajectory angles, and apparently it is difficult to directly use gyroscopes to achieve measurement. However, the trajectory angles can be estimated according to their definitions in the earth frame if velocity of a spinning body is determined. In other words, an alternative is to utilize some extra data relative to the velocity and estimate the trajectory angles. So, we address a backward process to use position from a satellite navigation system to assist to decouple the angular motion of spinning bodies for the past time.

Fig. 4. shows the geometrical relationship of trajectory angles and velocity. So, the position information by satellite navigation systems can be provided for differential computing of velocity during an updating interval, which can be further used to calculate trajectory angles and obtain trajectory angular velocity.

As the position data from satellite navigation systems is current, the velocity at the previous moment can be calculated by:

$$\begin{cases} v_x(t-1) = \dfrac{x(t) - x(t-1)}{\Delta t} \\ v_y(t-1) = \dfrac{y(t) - y(t-1)}{\Delta t} \\ v_z(t-1) = \dfrac{z(t) - z(t-1)}{\Delta t} \end{cases} \tag{7}$$

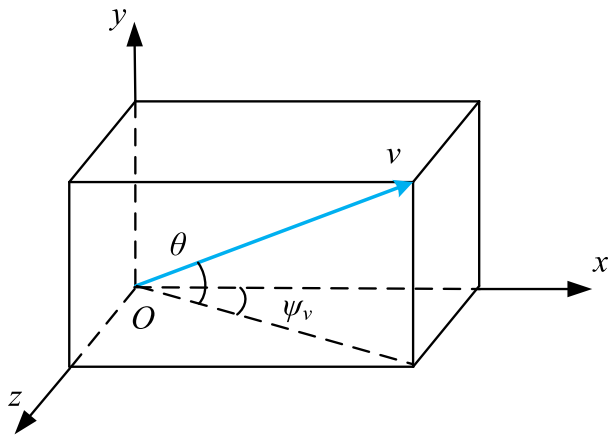

FIGURE 4. Geometrical relationship of trajectory angles and velocity.

where x, y and z represent the position of spinning bodies, t and $t-1$ represent the present moment and the previous moment, and Δt is the updating interval. By using (7), the trajectory angles can be calculated by:

$$\psi_v(t-1) = \arcsin \frac{v_z(t-1)}{\sqrt{v_x^2(t-1) + v_z^2(t-1)}} \tag{8}$$

or

$$\psi_v(t-1) = \arctan \frac{v_z(t-1)}{v_x(t-1)} \tag{9}$$

$$\theta(t-1) = \arctan \frac{v_y(t-1)}{\sqrt{v_x^2(t-1) + v_z^2(t-1)}} \tag{10}$$

By using (8) and (9), the differential forms of trajectory angles can be obtained approximatively as:

$$\dot{\psi}_v(t-2) = \frac{\psi_v(t-1) - \psi_v(t-2)}{\Delta t} \tag{11}$$

$$\dot{\theta}(t-2) = \frac{\theta(t-1) - \theta(t-2)}{\Delta t} \tag{12}$$

Based on (8) to (11), the angular velocity of trajectory angular motion at t-2 can be obtained as:

$$\omega_{ep}^{p}(t-2) = \begin{bmatrix} \dot{\psi}_v(t-2) \cdot c\theta(t-2) \\ \dot{\psi}_v(t-2) \cdot s\theta(t-2) \\ \dot{\theta}(t-2) \end{bmatrix} \tag{13}$$

Then, based on (5) and (6), the angular velocity of coning motion is derived as:

$$\omega_{pb}^{b}(t-2) = \omega_{eb}^{b}(t-2) \text{-} C_{p}^{b}(t-2) \cdot \omega_{ep}^{p}(t-2) \tag{14}$$

where $C_p^b(t-2)$ is updated by using $\omega_{pb}^b(t-3)$ to guarantee the real-time ability, and $\omega_{eb}^b(t-2)$ can be obtained directly from gyroscopes mounted in spinning bodies.

From (7) to (13), the angular velocity of coning motion at t-2 can be calculated with the assist of satellite navigation data, retrospectively. The backward decoupling process is shown in Fig. 5.

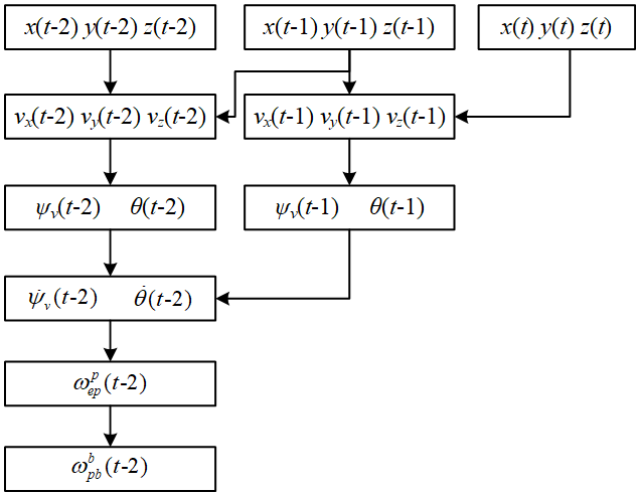

FIGURE 5. Backward decoupling process.

B. FORWARD DECOUPLING OF ANGULAR MOTION

Further analyzing the updating sequence above, it is certain that there is a real-time problem of decoupling angular motion while using the decoupled angular velocities before t-2 moment. In other words, we can only determine the attitude before t-1 moment by using the exact angular velocity. So, in order to determine attitude matrix and attitude of spinning bodies at t moment, it is necessary to calculate angular velocities of trajectory motion and coning motion at $t-1$. In contrast to the backward decoupling, we address a forward process to decouple angular motion of spinning bodies at the present moment.

The coning motion is much more high-frequency than the trajectory motion, so it is reasonable to assume that coning rotation speed is constant during a small update interval. Based on the backward decoupling, we can retrospect the coning angular velocities at t-2 and t-3, and then set up two adjacent orthogonal systems by using vector cross product [16]:

$$W_1 = \begin{bmatrix} \omega_{pb}^{b}(t3) \\ \omega_{pb}^{b}(t3) \otimes \omega_{pb}^{b}(t4) \\ \omega_{pb}^{b}(t-3) \otimes \left(\omega_{pb}^{b}(t-3) \otimes \omega_{pb}^{b}(t-4)\right) \end{bmatrix} \tag{15}$$

$$W_2 = \begin{bmatrix} \omega_{pb}^{b}(t2) \\ \omega_{pb}^{b}(t2) \otimes \omega_{pb}^{b}(t3) \\ \omega_{pb}^{b}(t-2) \otimes \left(\omega_{pb}^{b}(t-2) \otimes \omega_{pb}^{b}(t-3)\right) \end{bmatrix} \tag{16}$$

Apparently, the system W_1 follows the system W_2 over time, rotating at the same speed of coning motion. Figure 6 shows rotation relationship of the adjacent orthogonal systems.

The transfer relationship is expressed by:

$$W_2 = U(\Omega \cdot \Delta t) \cdot W_1 \tag{17}$$

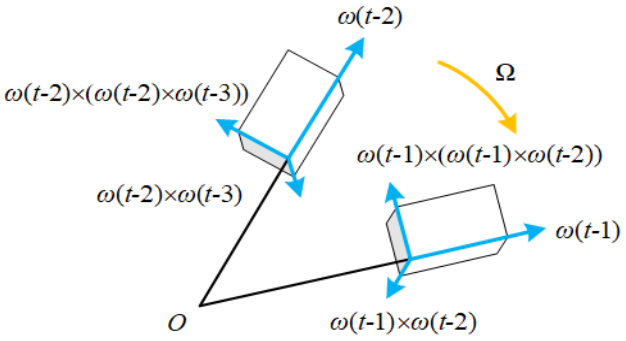

FIGURE 6. Rotation relationship of adjacent orthogonal systems.

where Ω is the rotation speed of coning motion, and $U(\Omega\cdot\Delta t)$ is the transfer matrix:

$$U(\Omega\cdot\Delta t)=\begin{bmatrix}1 & 0 & 0\\ 0 & c(\Omega\cdot\Delta t) & s(\Omega\cdot\Delta t)\\ 0 & -s(\Omega\cdot\Delta t) & c(\Omega\cdot\Delta t)\end{bmatrix} \tag{18}$$

According to the assumption of constant rotation speed of coning motion during a small update interval, the orthogonal system at $t-1$ moment is obtained by using the previous adjacent orthogonal systems:

$$W_3=W_2W_1^1W_2 \tag{19}$$

Then, we extract the angular velocity $\omega_{pb}^b(t1)$ from the orthogonal system W_3 by:

$$\omega_{pb}^b(t1)=W_3\{1\} \tag{20}$$

where $W_3\{1\}$ represents the first column of W_3. Based on (5), we estimate the trajectory angular velocity by:

$$\omega_{ep}^p(t1)=C_p^b(t1)\left(\omega_{eb}^b(t1)-\omega_{pb}^b(t1)\right) \tag{21}$$

According to (17) to (21), the forward decoupling process is summarized in Fig. 7.

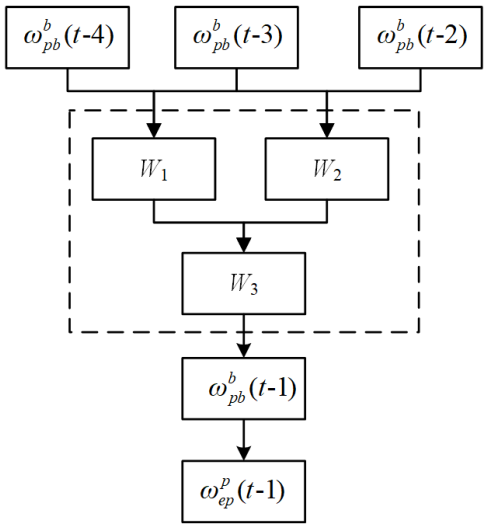

FIGURE 7. Forward decoupling process.

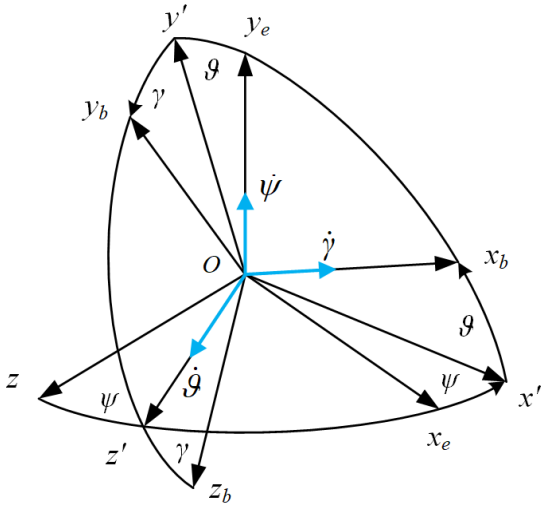

FIGURE 8. Relationship between the earth frame and the body frame.

IV. REAL-TIME ATTITUDE UPDATING ALGORITHM

Among conventional attitude updating algorithms, the rotation vector algorithm is the mainstream method, which directly uses angular increment or angular velocity to calculate rotation vector and update Euler attitude matrix. Usually, the Euler attitude angles that describe the relationship of body frame and earth frame are the pitch angle ϑ, the yaw angle ψ and the roll angle γ, as is shown in Fig. 8.

The definitions of these angles are to coincide the earth frame with the body frame by rotating along y axis, z axis and x axis successively. The attitude transfer matrix is obtained as:

$$C_e^b=\begin{bmatrix}c\vartheta c\psi & s\vartheta & -c\vartheta s\psi\\ -s\vartheta c\psi c\gamma+s\psi s\gamma & c\vartheta c\gamma & s\vartheta s\psi c\gamma+c\psi s\gamma\\ s\vartheta c\psi s\gamma+s\psi c\gamma & c\vartheta s\gamma & -s\vartheta s\psi s\gamma+c\psi c\gamma\end{bmatrix} \tag{22}$$

However, conventional attitude updating algorithms take no account of the coupling factor due to multi-angular motion. In this paper, attitude angles of different angular motion are updated respectively by using the decoupling angular velocities, and then calculate the real attitude of spinning bodies.

A. CONING ATTITUDE UPDATING

Through transformation of (4), we derive the differential function of cone attitude as:

$$\begin{bmatrix}\dot{\delta}_1\\ \dot{\delta}_2\\ \dot{\delta}_3\end{bmatrix}=\begin{bmatrix}0 & -c(\delta_1-\delta_3)/s\delta_2 & -s(\delta_1-\delta_3)/s\delta_2\\ 0 & -s(\delta_1-\delta_3) & c(\delta_1-\delta_3)\\ 1 & -c(\delta_1-\delta_3)\cdot t(\delta_2/2) & -s(\delta_1-\delta_3)\cdot t(\delta_2/2)\end{bmatrix}\times\begin{bmatrix}\omega_{pbx}^b\\ \omega_{pby}^b\\ \omega_{pbz}^b\end{bmatrix} \tag{23}$$

where $t(\cdot)$ represents $\tan(\cdot)$. By analyzing (23), there exists a singular problem while nutation angle is zero. So, we develop an updating algorithm based on rotation vector to expand

application of the cone frame and the cone attitude for coning motion existing during all the flight of spinning bodies.

The rotation vector is calculated by:

$$\phi(t) = \alpha(t) + \delta\phi(t) \tag{24}$$

$$\alpha(t) = \int_{t_m}^{t} \omega \cdot dt \tag{25}$$

$$\delta\phi(t) \approx \int_{t_m}^{t} \left(\frac{1}{2}\phi(t) \times \omega(t) + \frac{1}{12}\phi(t) \times (\phi(t) \times \omega(t)) \right) dt \tag{26}$$

where ω is short for the angular velocity of body frame with respect to the trajectory frame, namely the angular velocity of coning motion.

To guarantee the accuracy, the triple-cross-product term in (26) is taken into account. So, the rotation vector is calculated by [11]:

$$\hat{\phi}(t) = \sum_{i=1}^{N} \alpha_i(t) + \delta\phi_c(t) + \delta\phi_A(t) + \delta\phi_B(t) \tag{27}$$

$$\delta\phi_c(t) = \sum_{j=1}^{N-1} \sum_{i=j+1}^{N} k_{ij}[\Delta\alpha_{N+1-i} \times \Delta\alpha_{N+1-j}] \tag{28}$$

$$\delta\phi_A(t) = -\frac{1}{6} \sum_{i=1}^{N} \Delta\alpha_i(t) \times \sum_{j=1}^{N-1} \sum_{i=j+1}^{N} k_{ij}[\Delta\alpha_{N+1-i} \times \Delta\alpha_{N+1-j}] \tag{29}$$

$$\delta\phi_B(t) = \sum_{i=1}^{N} \sum_{j=1}^{N-1} \sum_{l=j+1}^{N} k_{N+i-1,N+j-1,N+l-1} \Delta\alpha_{N+1-i} \times [\Delta\alpha_{N+1-j} \times \Delta\alpha_{N+1-l}] \tag{30}$$

$$\Delta\alpha_{N+1-i} = \int_{t-\frac{i}{n}(t-t_{m-1})}^{t-\frac{i-1}{n}(t-t_{m-1})} \omega dt \tag{31}$$

$$\Delta\alpha_{N+1-j} = \int_{t-\frac{j}{n}(t-t_{m-1})}^{t-\frac{j-1}{n}(t-t_{m-1})} \omega dt \tag{32}$$

$$\Delta\alpha_{N+1-l} = \int_{t-\frac{l}{n}(t-t_{m-1})}^{t-\frac{l-1}{n}(t-t_{m-1})} \omega dt \tag{33}$$

where k_{ij} and $k_{N+i-1,\ N+j-1,\ N+l-1}$ are the calculation coefficients determined under coning environment, and N represents sub sample number.

The cone transfer matrix is updated by:

$$C_p^b(t) = \Delta C\,(t)\, C_p^b(t-1) \tag{34}$$

$$\Delta C\,(t) = I + f_1\,(\phi(t))\,(\phi(t)\times) + f_2\,(\phi(t))\,(\phi(t)\times)^2 \tag{35}$$

$$f_1\,(\phi(t)) = \frac{\sin|\phi(t)|}{|\phi(t)|} = \sum_{k=1} (-1)^{k-1} \frac{|\phi(t)|^{2(k-1)}}{(2k-1)!} \tag{36}$$

$$f_2\,(\phi(t)) = \frac{1-\cos|\phi(t)|}{|\phi(t)|^2} = \sum_{k=1} (-1)^{k-1} \frac{|\phi(t)|^{2(k-1)}}{(2k)!} \tag{37}$$

TABLE 1. Real value of precession angle.

c_{21}	c_{31}	δ_1
+	+	$\hat{\delta}_1$
-	-	$\hat{\delta}_1+\pi$
-	+	$\hat{\delta}_1+\pi$
+	-	$\hat{\delta}_1+2\pi$

TABLE 2. Real value of spin angle.

c_{12}	c_{13}	δ_1
-	+	$\delta_1+\hat{\delta}_3$
+	+	$\delta_1+(\hat{\delta}_3+\pi)$
+	-	$\delta_1+(\hat{\delta}_3+\pi)$
-	-	$\delta_1+(\hat{\delta}_3+2\pi)$

$$\phi(t)\times = \begin{bmatrix} 0 & -\phi_z & \phi_y \\ \phi_z & 0 & -\phi_x \\ -\phi_y & \phi_x & 0 \end{bmatrix} \tag{38}$$

where ϕ_x, ϕ_y, ϕ_z are elements of the vector increment. According to (3), the nutation angle, the precession angle and the spin angle are calculated by:

$$\hat{\delta}_1 = \arctan\left(c_{21}/c_{31}\right) \tag{39}$$

$$\delta_2 = \arccos\left(c_{11}\right) \tag{40}$$

$$\delta_1 - \hat{\delta}_3 = -\arctan\left(c_{12}/c_{13}\right) \tag{41}$$

where $\hat{\delta}_1$ and $\hat{\delta}_3$ are fake values of the precession angle δ_1 and the spin angle δ_3, respectively. The real values of δ_1 and δ_3 are determined according to Table 1 and Table 2. It is noted that the precession angle should be updated before the spin angle.

B. TRAJECTORY ATTITUDE UPDATING

The updating processes of trajectory attitude before and after $t-1$ are different. The attitude at t moment is updated by using trajectory angular velocity at $t-1$ moment whereas the trajectory attitude before $t-1$ is updated directly by using data from satellite navigation. According to (2), we extract the differential values of trajectory angles by:

$$\dot{\theta}(t-1) = \omega_{ep}^{p}(t-1)\,\{3\} \tag{42}$$

$$\dot{\psi}_v(t-1) = \frac{\omega_{ep}^{p}(t-1)\,\{2\}}{s\theta(t-1)} \tag{43}$$

Then, we update the trajectory attitude by:

$$\theta(t) = \int_{t-1}^{t} \dot{\theta}(t-1)dt \tag{44}$$

$$\psi_v(t) = \int_{t-1}^{t} \dot{\psi}_v(t-1)dt \tag{45}$$

We can further update the trajectory transfer matrix at t moment by using (1).

TABLE 3. Real value of yaw angle.

$C_e^b[1,1]$	$C_e^b[3,1]$	ψ
+	+	$\hat{\psi}$
-	-	$\hat{\psi}+\pi$
-	+	$\hat{\psi}+\pi$
+	-	$\hat{\psi}+2\pi$

TABLE 4. Real value of roll angle.

$C_e^b[2,2]$	$C_e^b[2,3]$	γ
-	+	$\hat{\gamma}$
+	+	$\hat{\gamma}+\pi$
+	-	$\hat{\gamma}+\pi$
-	-	$\hat{\gamma}+2\pi$

C. BODY ATTITUDE UPDATING

According to continuous coordinate transferring, the attitude matrix is expressed as:

$$C_e^b(t) = C_p^b(t) \cdot C_e^p(t) \tag{46}$$

The Euler attitude angles are calculated by:

$$\vartheta(t) = \arcsin\left(C_e^b(t)[1,2]\right) \tag{47}$$

$$\hat{\psi}(t) = -\arctan\frac{C_e^b(t)[1,3]}{C_e^b(t)[1,1]} \tag{48}$$

$$\hat{\gamma}(t) = -\arctan\frac{C_e^b(t)[3,2]}{C_e^b(t)[2,2]} \tag{49}$$

where $C_e^b(t)[i,j]$ represents the element at i th row, j th column of $C_e^b(t)$, $\hat{\psi}(t)$ and $\hat{\gamma}(t)$ are fake values of the yaw angle and the roll angle. The real values of ψ and γ are determined according to Table 3 and Table 4.

V. SIMULATION AND EXPERIMENT

A. SIMULATION AND ANALYSIS

In order to verify the validity of the angular motion decoupling and attitude updating algorithm, simulations are carried out successively under different angular motion conditions, different self-spin speed conditions and different linear velocity conditions. The attitude updating algorithm chooses N =3, and the corresponding coefficients including k_{ij} and $k_{N+i-1,N+j-1,N+l-1}$ are shown in Table 5. The update time is 0.5ms and simulation time is 60s.

1) DIFFERENT ANGULAR MOTION CONDITIONS

Four cases of different angular motion conditions are designed, and the changing regularity of time-varying parameters are shown in Table 6. We assume that the spinning body has other same initial parameters such as the launching speed 400m/s, the spinning speed 1800°/s, the nutation angle 5°, the spin angle 0° and the drift angle 0° in each case. Additionally, the second derivative of the trajectory drift angle is assumed to be 0.000573°/s to make trajectories change nonlinearly. The frequency of satellite navigation is assumed to be 20Hz, and the trajectories of the spinning body are shown in Fig. 9.

TABLE 5. Coefficients of the attitude updating algorithm.

Coefficients	Value
k_{11}	0.45
k_{12}	0.675
k_{112}	-1.2229
k_{212}	1.0021
k_{312}	0.0396
k_{123}	-0.3771
k_{223}	1.2354
k_{323}	-0.3396
k_{113}	1.1562
k_{213}	-0.7625
k_{313}	0.0000

TABLE 6. Angular motion conditions of the spinning body.

Parameters	θ (°)	$\dot{\theta}$ (°/s)	$\dot{\psi}_v$ (°/s)	$\dot{\delta}_1$ (°/s)	$\dot{\delta}_2$ (°/s)
Case 1	30	1.0001	0.0573	90	0.01146
Case 2	45	1.4954	0.1146	180	0.05730
Case 3	60	1.9996	0.1719	360	0.11460
Case 4	70	2.3319	0.2292	540	0.22920

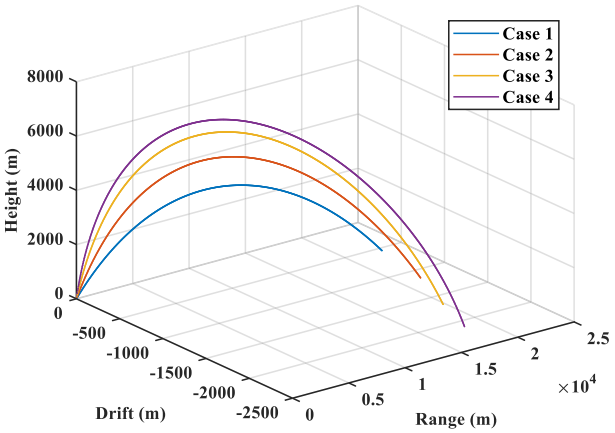

FIGURE 9. Position of the spinning body in different angular motion conditions. Range, height and drift are corresponding to x, y and z of the earth frame.

Fig. 10 shows triaxial angular velocities in four cases. Under these conditions, the attitude error is varying to diverge quickly, which is magnified from 55s to 60s in Fig. 11. The maximum amplitude of the roll angle error is 54.92°, the maximum amplitude of the yaw angle error is 1.16°, and the maximum amplitude of the pitch angle error is 0.17°. Based on Fig 11, it is pretty sure

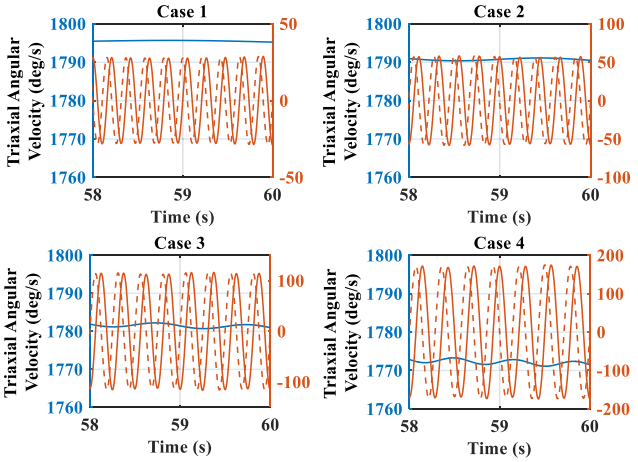

FIGURE 10. Triaxial angular velocities in different angular motion conditions.

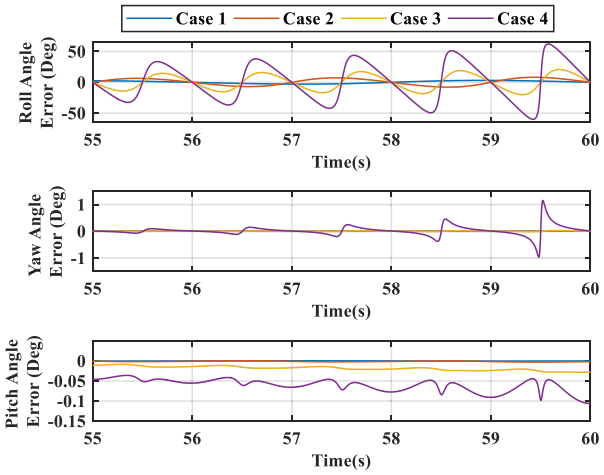

FIGURE 11. Attitude induced error of the conventional algorithm.

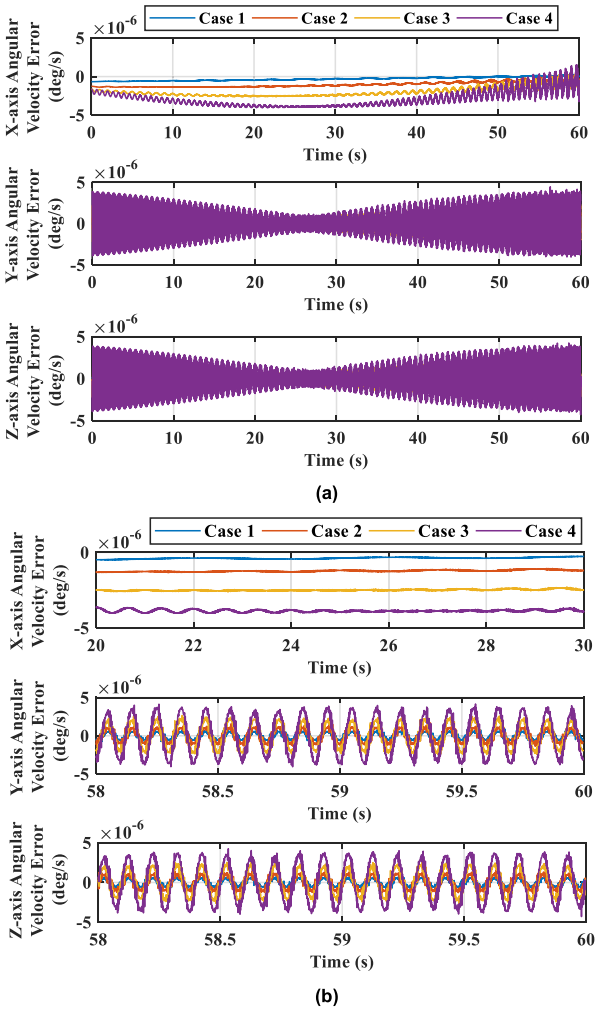

FIGURE 12. Estimating error of the cone angular velocity in different angular motion conditions. (a) the whole varying during 0s∼60s; (b) the biggest parts of estimating error.

that the coupling of angular motion affects conventional algorithms to generate attitude error, and it is becoming bigger if the angular motion condition is much fiercer.

The satellite navigation frequency is much lower than the algorithm update frequency, so we need to process the position data by using forward interpolation to generate one hundred points and match the frequency of gyroscopes. So, the position update time is enhanced to be 0.5ms. Although some small errors exist in interpolation, this does not have much effect on decoupling. This is because navigation data provide position of the center of mass of the projectile, and the swing effect of the forepart could be brought into position data. The estimating error of the cone angular velocity and the magnified parts are shown in Fig. 12. The angular velocity error of x-axis obtains its biggest at the peak of trajectory and vibrates the most at the end. The biggest parts of y-axis and z-axis happen at the end. In the magnified drawing, the estimating error is no bigger than 5e-6 degree per second for 60s. The reason why using satellite data can estimate angular velocity accurately is that the simulation conditions are ideal, there is no coupled random angular vibration as well. Even so, it is certain that the estimating error has increasing tendency if the angular motion becomes complex.

Then, we use angular velocity estimated to update cone attitude, and the cone attitude error shown in Fig. 13 is no greater than 0.2°. The attitude error is oscillating but not diverging. It is different from that of the conventional algorithm, because this attitude error is mainly originated from the transformation of rotation vector to cone attitude matrix. Fig. 14 shows the attitude error of the real-time attitude updating algorithm, and the roll angle is replaced by the spin angle. It is seen that the amplitude of attitude error is no greater than 0.7°, which is much smaller than that of the conventional algorithm. The error is caused by the propagation of the rotation vector error to attitude matrix, and it is hard to avoid up to now.

2) DIFFERENT SELF-SPIN SPEED CONDITIONS

To examine the effect of high spinning speed on the real-time angular decoupling and attitude updating algorithm,

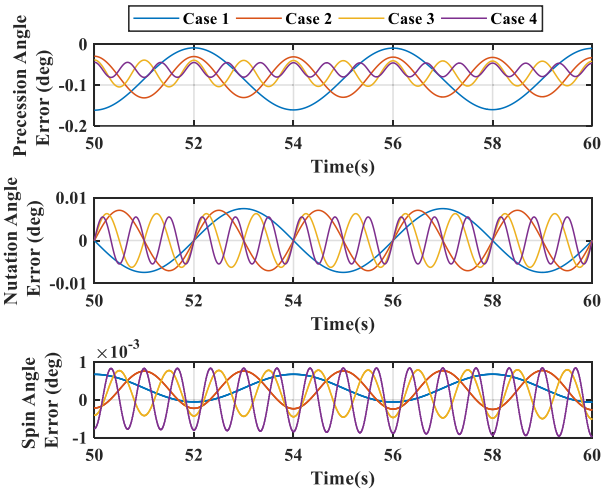

FIGURE 13. Cone attitude error in different angular motion conditions.

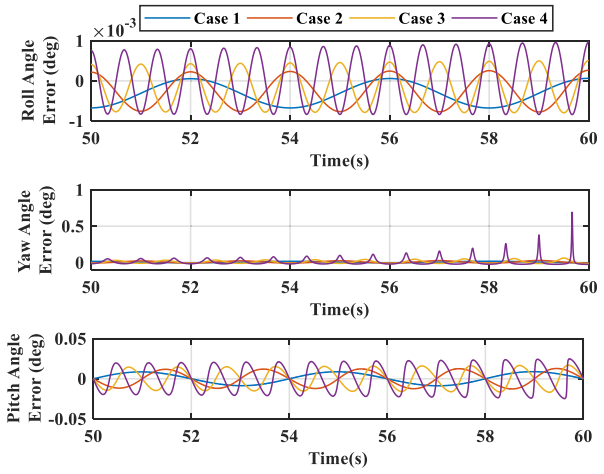

FIGURE 14. Attitude error of the real-time angular decoupling and attitude updating algorithm in different angular motion conditions.

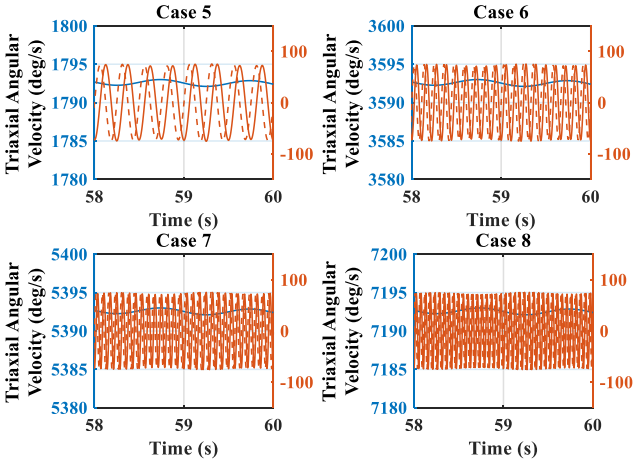

FIGURE 15. Angular velocity in different spinning speed conditions.

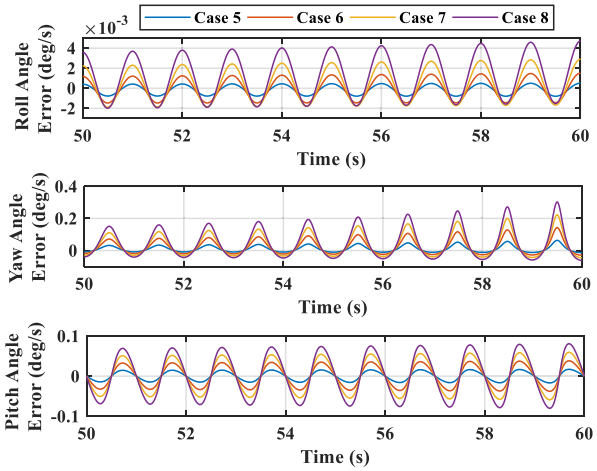

FIGURE 16. Attitude error of the real-time angular decoupling and attitude updating algorithm in different spinning speed conditions.

we choose the angular motion condition in case 3 and set the self-spin speed to be 1800°/s, 3600°/s, 5400°/s and 7200°/s.

Fig. 15 shows the angular velocity in different spinning speed conditions, and the alternate frequencies of y axis and z axis become higher. The attitude error of the real-time angular decoupling and attitude updating algorithm is shown in Fig. 16, and the amplitude is enlarged the same times as the self-spin speed, and it has diverging tendency. It is certain that the self-spin condition affects attitude oscillating error, which needs to be considered seriously.

3) DIFFERENT LINEAR VELOCITY CONDITIONS

To examine the effect of high linear velocity of spinning bodies on the real-time attitude updating algorithm proposed in this paper, we also choose the angular motion condition in case 3 and set the linear velocity to be 400m/s, 600m/s, 800m/s and 1000m/s. The frequencies of satellite navigation and the interpolation remain unchanged.

Fig. 17 shows position of the spinning body in different linear velocity conditions. Using the same method proposed in this paper, the estimating error of cone angular velocity in different linear velocity condition is not becoming bigger but has the similar value from case 10 to case 12, as is shown in Fig. 18. This is because high linear speed makes trajectory change quite small during each update time. In other words, increasing launching speed has a little harmful effect on using satellite navigation and keeping accuracy though the whole difference is propagated into attitude error of the real-time angular decoupling and attitude updating algorithm, as is shown in Fig. 19.

From the simulation results above, it is certain that the validity of the real-time angular decoupling and attitude updating algorithm proposed in this paper is proved to be able to decouple angular motion, update attitude of spinning bodies in real time and avoid the big effect of coupled angular motion on conventional algorithms.

B. EXPERIMENT AND ANALYSIS

An off-line flight data is extracted from a real flight of a 130mm projectile with complex angular motion to make

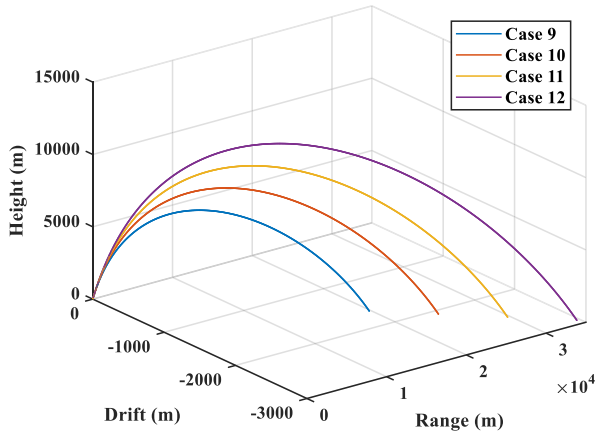

FIGURE 17. Position of the spinning body in different linear velocity conditions.

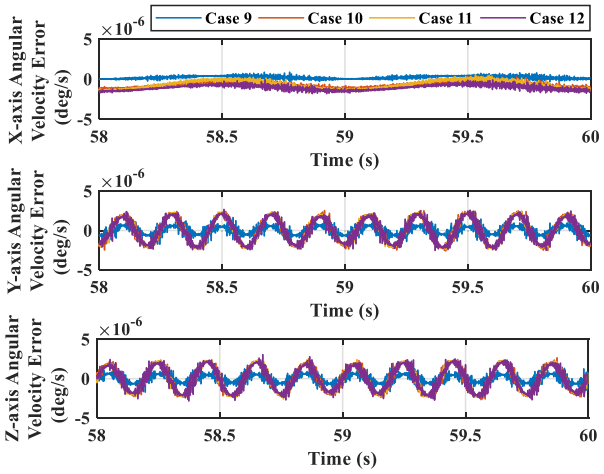

FIGURE 18. Estimating error of the cone angular velocity in different linear velocity conditions.

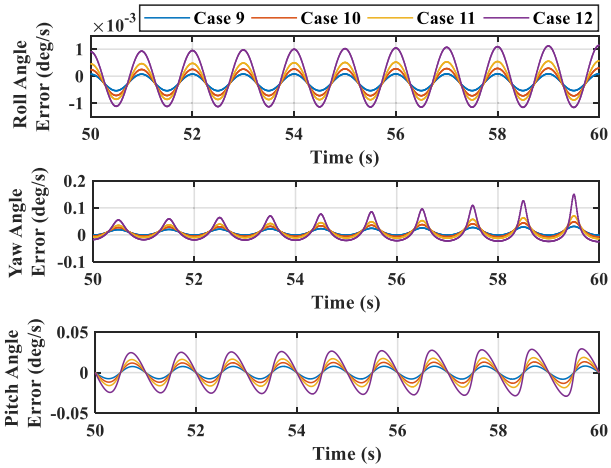

FIGURE 19. Attitude error of the real-time angular decoupling and attitude updating algorithm in different linear velocity conditions.

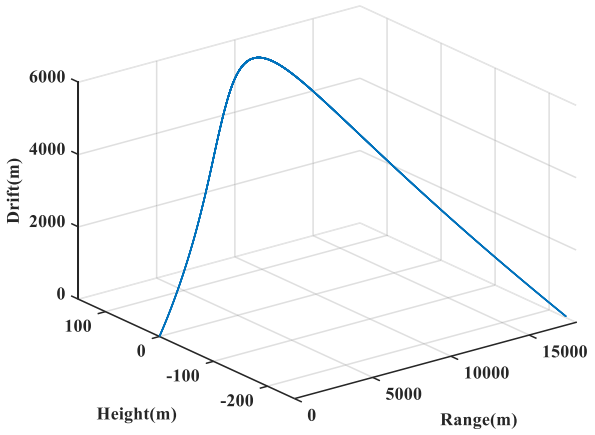

FIGURE 20. Position of the projectile.

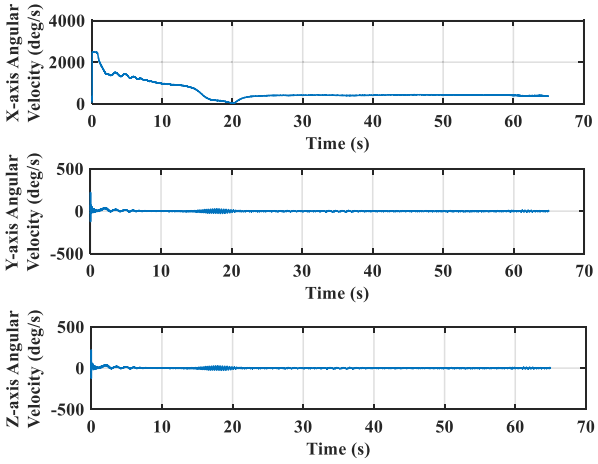

FIGURE 21. Angular velocity of the projectile.

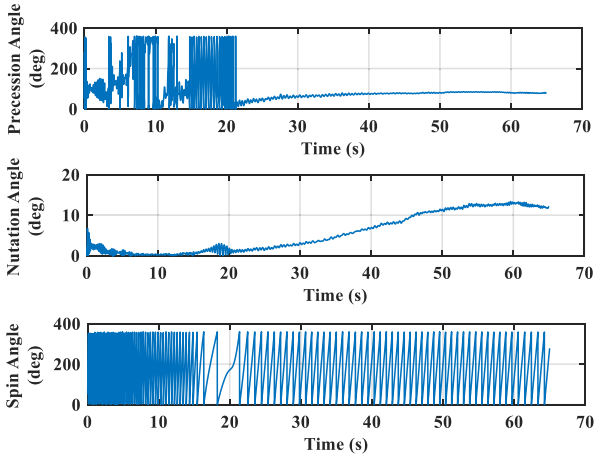

FIGURE 22. The decoupled cone attitude.

engineering analysis for the availability of the real-time angular decoupling and attitude updating algorithm. The projectile is launched with muzzle velocity 650m/s, and the initial attitude is followed as below, the roll angle 30°, the yaw angle is 0° and the pitch angle is 45°. The satellite navigation system is integrated in the center of mass of the projectile, and its updating frequency is 20Hz. The main performance parameters of gyroscopes for high spinning speed are shown in Table 7. The update time is 1ms and the flight time is 65s.

The position of the projectile is shown in Fig. 20. We employ the same interpolation process to match the

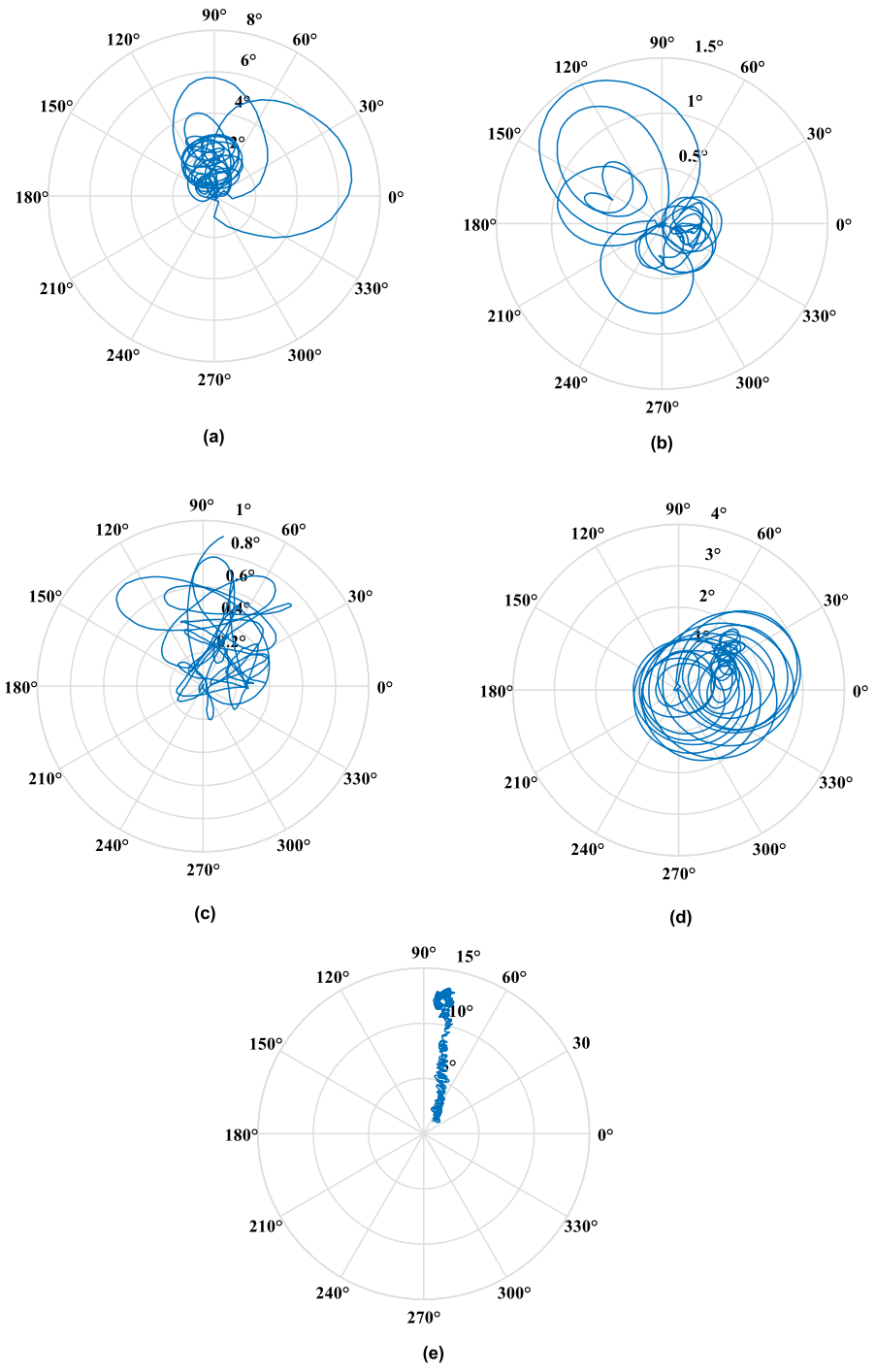

FIGURE 23. Varying process of coning motion. (a) 0s∼5s; (b) 5s∼10s; (c) 10s∼15s; (d) 15s∼25s. (e) 25s∼65s.

frequency of gyroscopes. Fig. 21 shows the angular velocity of the projectile, and the maximum value of x-axis is 2483.38°/s. From 0s to 10s and from 17s to 22s, the x-axis angular velocity reduces and tends to be the minimum value, but the other two axes have angular velocities of the different frequency through comparison of triaxial angular velocity. The apparent mismatching and fluctuations indicate the projectile experiences complex angular motion.

By using the decoupled angular velocity of coning motion, the cone attitude is calculated and shown in Fig. 22, and the varying process of coning motion is shown in Fig. 23. During 0s∼5s, the nutation angle varies frequently from 7° to 1.5° after lunching, and this complex process explains that the first change of aerodynamic configurations has significant effect on flight. During 5s∼15s, the projectile becomes stable gradually and flies placidly. This process proves that the

TABLE 7. Main performance parameters of the gyroscopes.

Parameters	X-Axis Gyroscope	Y-Axis Gyroscope	Z-Axis Gyroscope
Range	±3600°/s	±540°/s	±540°/s
Bias Instability	9.17°/h	5.81°/h	4.99°/h
Non-Linearity	0.03%	0.02%	0.02%
Noise density	0.14°/s/√Hz	0.05°/s/√Hz	0.05°/s/√Hz
Update rate	200Hz	200Hz	200Hz

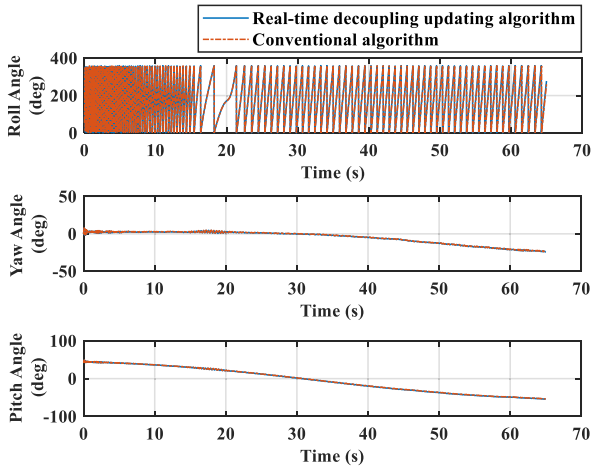

FIGURE 24. Comparison of attitude by the real-time decoupling updating algorithm and the conventional algorithm.

TABLE 8. Attitude differences.

δ_3-γ	$\Delta\psi$	$\Delta\vartheta$
16.83°	1.34°	1.48°

superiority of high spinning speed keeps fluctuation from diverging. After 15s, the projectile is affected by the second change of aerodynamic configurations and forced to have a fierce coning motion with the nutation no greater than 3.5°. But 5s later, it goes into a stable condition till 25s by adjusting of the control system. From 25s to 65s, nutation angle is increasing without apparent precession angle, which means the projectile flies with a big angle. Meanwhile, a fact can be seen that the coning motion is not a single circle but a double circle, especially in Fig. 23(b) and Fig. 23(d). Actually, different forms of coning motion exist during the spinning body flying, but it is very difficult to decouple them. Based on Fig. 22 and Fig. 23, it is certain that the complicated angular motion of the projectile is decoupled to a certain extent.

The attitude differences of the real-time attitude updating algorithm and the conventional algorithm are shown in Fig. 24, and an apparent distinction is calculated in Table 8. The roll angle error is 16.83° whereas the pitch angle error and the yaw angle error are 1.34° and 1.48° respectively.

Objectively speaking, whichever level of gyroscopes would not affect accuracy of attitude updating algorithms, and attitude error that is not apparent or big enough could be covered up. However, attitude error could be magnified by varying coupled angular motion, especially oscillating attitude error would be cut off and propagated to the next update cycle when angular motion is changing unexpectedly. Besides, it is hard to acquire the real attitude of the projectile and apply gyroscopes of much higher-level accuracy to measure high spin velocity in real flight. Under this circumstance, any reasonable and convergent change can be regarded as improvements based on the simulation results above, if we input the same gyroscope data and navigation data to the real-time attitude updating algorithm and the conventional algorithm. Therefore, this indicates that the real-time angular motion decoupling and attitude updating method is helpful and available for engineering application.

VI. CONCLUSION

In order to find out a valid engineering method to reduce the coupled effect of complex angular motion on conventional attitude algorithms and obtain real attitude of spinning bodies, this paper proposes a real-time angular motion decoupling and attitude updating method by using satellite navigation data. A compositive model of angular motion is built by combing trajectory motion and coning motion, which is convenient to understand the trait of angular velocity and lay a necessary basis for decoupling. In the decoupling process of angular motion, a backward decoupling process is addressed with the help of satellite navigation data to retrospect the exact velocity and attitude, and a forward decoupling angular process is addressed to estimate real-time angular velocity by the relationship of adjacent orthogonal systems of previous angular velocity. A real-time attitude updating algorithm is presented to calculate coning attitude, trajectory attitude and real attitude of spinning bodies by using the real-time angular velocity, especially, the updating process of the cone attitude by vector rotation is presented. Simulations with different conditions are carried out to show the effect on the conventional algorithm and verify the validity of this method, and flight data of a projectile are used to implement decoupling and analyzing of angular motion, which also proves availability in engineering application.

In the future work, we will focus on measuring angular velocity and attitude initial alignment of spinning bodies.

REFERENCES

[1] S. Zhang, X. Li, and Z. Su, "Measuring and solving real coning motion of spinning carriers," *Proc. Inst. Mech. Eng., G, J. Aerosp. Eng.*, vol. 230, no. 13, pp. 2369–2378, 2016.
[2] S. Zhang, X. Li, and Z. Su, "Cone algorithm of spinning vehicles under dynamic coning environment," *Int. J. Aerosp. Eng.*, vol. 2015, Nov. 2015, Art. no. 904913.
[3] J. E. Bortz, "A new mathematical formulation for strapdown inertial navigation," *IEEE Trans. Aerosp. Electron. Syst.*, vol. AES-7, no. 1, pp. 61–66, Jan. 1971.
[4] P. G. Savage, "Coning algorithm design by explicit frequency shaping," *J. Guid. Control Dyn.*, vol. 33, no. 4, pp. 1123–1132, 2010.
[5] R. B. Miller, "A new strapdown attitude algorithm," *J. Guid., Control, Dyn.*, vol. 6, no. 4, pp. 287–291, 1983.
[6] J. G. Lee, J. G. Mark, and D. A. Tazartes, "Extension of strapdown attitude algorithm for high-frequency base motion," *J. Guid., Control, Dyn.*, vol. 13, no. 4, pp. 738–743, 1990.

[7] M. B. Ignagni, "Efficient class of optimized coning compensation algorithms," *J. Guid., Control, Dyn.*, vol. 19, no. 2, pp. 424–429, 1996.
[8] C. Tang and X. Chen, "A class of coning algorithms based on a half-compressed structure," *Sensors*, vol. 14, no. 8, pp. 14289–14301, 2014.
[9] Y. F. Jiang and Y. P. Lin, "Improved strapdown coning algorithms," *IEEE Trans. Aerosp. Electron. Syst.*, vol. 28, no. 2, pp. 484–490, Apr. 1992.
[10] P. G. Savage, "Explicit frequency-shaped coning algorithms for pseudo-coning environments," *J. Guid. Control Dyn.*, vol. 34, no. 3, pp. 774–782, 2015.
[11] M. Wang, W. Wu, J. Wang, and X. Pan, "High-order attitude compensation in coning and rotation coexisting environment," *IEEE Trans. Aerosp. Electron. Syst.*, vol. 51, no. 2, pp. 1178–1190, Apr. 2015.
[12] M. Wang, W. Wu, and X. He, "Higher-order rotation vector attitude updating algorithm," *J. Navigat.*, vol. 72, no. 3, pp. 721–740, 2019.
[13] Y. Wu, "RodFIter: Attitude reconstruction from inertial measurement by functional iteration," *IEEE Trans. Aerosp. Electron. Syst.*, vol. 54, no. 5, pp. 2131–2142, Oct. 2018.
[14] Y. Wu, Q. Cai, and T.-K. Truong, "Fast RodFIter for attitude reconstruction from inertial measurements," *IEEE Trans. Aerosp. Electron. Syst.*, vol. 55, no. 1, pp. 419–428, Feb. 2019.
[15] F. Liu, Z. Su, Q. Li, and H. Zhao, "Angular motion decoupling and attitude determination based on high dynamic gyro," *IEEE Access*, vol. 7, pp. 14308–14322, 2019.
[16] R. P. Patera, "Attitude propagation for a slewing angular rate vector," *J. Guid., Control, Dyn.*, vol. 33, no. 6, pp. 1847–1855, 2010.

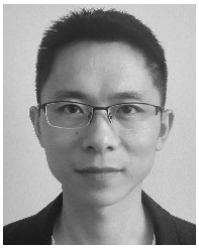

SHUANGBIAO ZHANG received the B.S. degree in mechatronics from the Department of Mechatronics Engineering, Henan University of Science and Technology, Luoyang, China, in 2007, and the Ph.D. degree from the Department of Aerospace Engineering, Beijing Institute of Technology, Beijing, China, in 2016. He is currently a Researcher with Beijing Information Science and Technology University. His research interests include high dynamic inertial sensors, attitude algorithms, and intelligent navigation of high spinning bodies.

ZHONG SU received the B.S. and M.S. degrees in automatic control from the Department of Automation, Beijing Institute of Technology, Beijing, China, in 1983 and 1989, respectively, and the Ph.D. degree from the Beijing Institute of Vacuum Electronics Technology, Beijing, in 1998. He is currently a Professor with Beijing Information Science and Technology University. His research interests include inertial devices, novel gyro sensors, high-dynamic navigation and control, integrated navigation, and wisdom perception technology.

XINGCHENG LI received the B.S. and M.S. degrees in mechatronics from the Department of Mechatronics Engineering, Xi'an University of Technology, Xi'an, China, in 1992 and 1995, respectively, and the Ph.D. degree from the Department of Aerospace Engineering, Beijing Institute of Technology, Beijing, China, in 2012. He is currently an Associate Professor with the Beijing Institute of Technology. His research interests include flight control systems, inertial measurement, and integrated navigation.